CONCEPT OF A POLARIZED POSITRON SOURCE FOR CEBAF

S. Habet[1,2], Y. Roblin[2], R.M. Bodenstein[2], S.A. Bogacz[2], L. Fanglei[2], J. Grames[2], A. Hofler[2], R. Kazimi[2], M. Poelker[2], A. Seryi[2], R. Suleiman[2], A. Sy[2], D. Turner[2], A. Ushakov[1], C.A. Valerio-Lizarraga[3], E. Voutier[1]

[1]*Université Paris-Saclay, CNRS/IN2P3/IJCLab, 91405 Orsay, France*

[2]*Thomas Jefferson National Accelerator Facility, Newport News, VA 23606, USA*

[3]*Universidad Autónoma de Sinaloa, 80010 Culiacáan, México*

Abstract

Polarized and unpolarized positron beams are essential for the future hadronic physics experimental program at the Thomas Jefferson National Accelerator Facility (JLab). The main challenge is to produce high duty-cycle and high intensity polarized positron beams. The JLab positron source uses the Polarized Electrons for Polarized Positrons (PEPPo) technique to create either a low intensity, high polarization positron beam (I > 100 nA, P=60%), or a high intensity unpolarized positron beam (I > 3 μA), from an intense highly polarized electron beam (I=1 mA, P=90%). The current design involves a new injector dedicated to positron production, collection, and shaping suitable for acceleration through the Continuous Electron Beam Accelerator Facility (CEBAF). The optimization of the layout and the performance of the positron source are explored in this paper.

INTRODUCTION

Positron beams can be used to probe physics phenomena. For instance, high energy beams allow to investigate the structure of nuclei while low energy beams access the distribution of electrons inside materials [1]. One interest at JLab is the study of the partonic structure of the nucleon from the scattering of highly polarized electron and positron beams. For instance, the comparison between the two beam species allows to isolate the different components of the deeply virtual Compton scattering cross section, and provides more pertinent and sensitive experimental observables [2, 3].

In this context, we may refer to the PEPPo experiment [4, 5], which demonstrated at the CEBAF injector the efficient polarization transfer from longitudinally polarized electrons to positrons [6]. Initial beam electrons generate elliptical polarized photons within a tungsten target via bremsstrahlung. These polarized photons then create in the same target positron and electron pairs. The main concern of the JLab positron project is to generate high-duty cycle longitudinally polarized positron beams from a 120 MeV/c electron beam with as high as possible an efficiency. The essential difficulty is to keep a high positron efficiency all along the collection and transport line of the positrons to the main accelerator, and to permit polarized or unpolarized dual operation with a small momentum dispersion delivered to experimental halls. The positron injector layout design, the target thickness optimization, and the positron beam optics are described in the following sections.

POSITRON INJECTOR LAYOUT

The positron injector is designed to provide an efficient number of positrons suitable for CEBAF injection. The transverse and longitudinal dynamics of the positron beam are optimized to stay within the acceptance limits. A positron collection system composed of high magnetic field lenses [7] is essential to decrease the large transverse momentum spread at the target exit. A conceptual layout of the injector is shown in Fig. 1. A moderate energy electron beam interacts within a tungsten target (T) to produce positrons that are collected with an Adiabatic Matching Device (AMD). A four quadrupoles matching section (MS) and a magnetic chicane (CP) select further the central momentum and the momentum bite of the positron population. A decelerating/accelerating section (DeAc) reduces then the momentum dispersion. Finally, a chirping cavity (ChC) correlates the momentum dispersion with the positron time-of-flight, and a second chicane (CC) compresses the positron bunch length to match with the CEBAF injection acceptance. We have determined the maximum bunch length acceptance is 4 ps, and our strategy is to further reduce this towards the nominal 12 GeV e- bunch length as possible, of 0.3 ps through compression techniques.

POSITRON TARGET OPTIMIZATION

Geant4 [8] simulations are used to optimize the positron production considering a 120 MeV/c electron beam 100% longitudinally polarized hitting a tungsten target. The analysis of simulated data follows the evolution of the positron production efficiency ϵ and of the Figure-of-Merit FoM=$\epsilon P_{e^+}^2$ as function of the target thickness. ϵ is the quantity of interest for an unpolarized positron source. The FoM further combines the average polarization to maximize the statistical precession of an experiment in the minimum amount of time. This investigation aims to optimize the target thickness for the production of unpolarized and polarized positrons. The Fig. 2 shows ϵ (left) and FoM (right) simulations for a 4 mm thick target, within a selected momentum bite $\Delta p/p$=±10% at each central momentum p_0 and within the angular acceptance $\Delta\theta_{e^+}$. The efficiency decreases when the angular aperture decreases, describing a large positron momentum spread in the transverse plane. The essential difference between unpolarized and polarized operation modes is the positron energy to be selected for optimum collection: about a sixth of the primary electron beam energy for optimized efficiency, and a half for optimized FoM. The maximum value

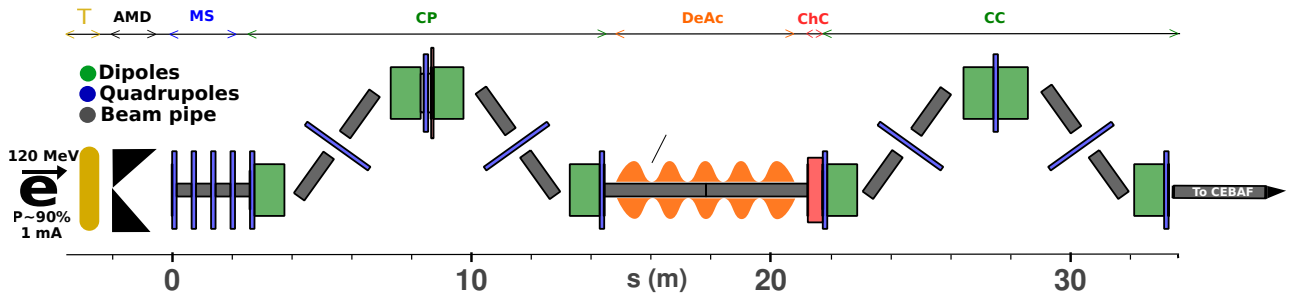

Figure 1: Conceptual layout of the positron injector for CEBAF.

of ϵ and FoM determines the optimum target thickness. At 120 MeV/c, it is about 4 mm, however, depending on the angular acceptance and the operation mode. The absolute value of ϵ and FoM are strongly affected by the angular acceptance and the momentum bite. These define the main parameters of the optimization of the positron injector.

PRELIMINARY CHARACTERIZATION

Momentum selection

Fig. 2 establishes the momentum selection procedure for unpolarized and polarized mode operation which is chosen at the p_0 peak value of the efficiency or the FoM. In order to select the corresponding positron yield a conversion of the momentum dispersion from the longitudinal plane $(\delta p/p, z)$ to the transverse plane $(\delta p/p, z)$ was explored. A magnetic chicane is designed from two opposite doglegs constituted of dipoles centered around p_0. Since the positron beam is polychromatic, the dogleg will allow to reach the maximum dispersion at its exit. The dispersion generated by each dipole is calculated from the expression [9]

$$D(s) = S(s) \int_0^s \frac{1}{\rho} C(t)\, dt \; - \; C(s) \int_0^s \frac{1}{\rho} S(t)\, dt \quad (1)$$

where $C(s)$ and $S(s)$ are the parameters of the 2×2 dipole transfer matrix. The dispersion function for each dipole can be expressed as

$$D = \rho \quad 1 - \cos \quad \frac{L}{\rho} \quad (2)$$

which quantifies the dogleg action on the beam in the $(x, \delta p/p)$ plane. The positron beam envelope evolution along the dogleg is shown on Fig. 3. At the dogleg entrance (blue), the transverse coordinates x do not correlate with the momentum dispersion. At the middle of the chicane, the positron distribution (red) exhibits an essential correlation between x and $\delta p/p$. Therefore, a collimator centered at $x = 0$ with appropriate aperture selects a given $\Delta p/p$ of positron momentum. The distribution at the exit of the collimator (green) corresponds to a 5 mm radius collimator, selecting a $\pm 10\%$ of positron momentum.

Beam size

Maximizing the positron selection efficiency after the collimator implies for the smallest beam size at the middle of the chicane. Thus a focusing-defocusing (FODO) lattice is introduced along the chicane. It consists of three quadrupoles, the first and the third are placed respectively at the entrance and exit legs of the chicane, the second at the middle of the chicane. The FODO aims at making a periodic β-function to obtain a minimum transverse beam size at the middle of the chicane. The periodicity condition requires $\beta_{out} = \beta_{in}$

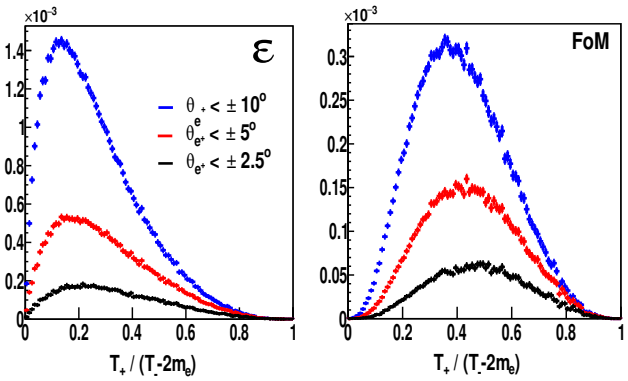

Figure 2: Positron production characteristics at 120 MeV/c off a 4 mm tungsten target, considering different angular acceptances and a $\pm 10\%$ momentum bite.

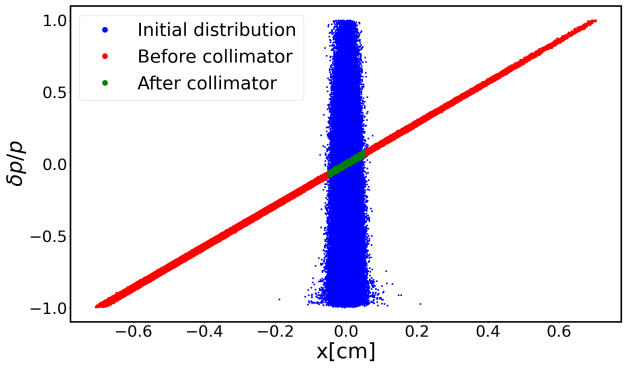

Figure 3: $(\delta p/p, x)$ positron distributions at the entrance (blue) and middle of the chicane (red), and at the collimator exit (green).

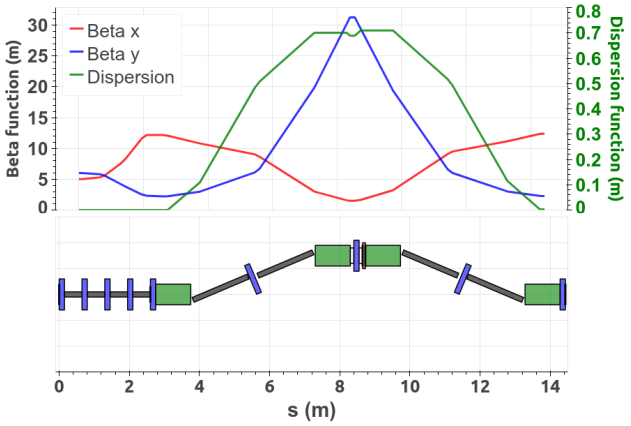

Figure 4: Variation of the optical β-function along the chicane.

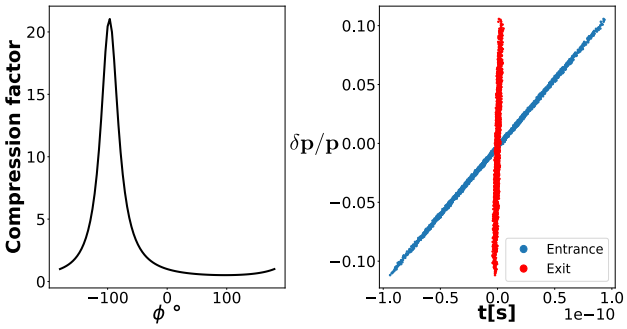

Figure 5: Variation of the compression factor vs the cavity phase advance (left), and full compression of the longitudinal beam length (right).

where β's are the positron beam twiss functions related to the transverse beam size at the entrance (in) and the exit (out) of the chicane. The evolution of the β-function along the chicane is shown in Fig. 4. The matching section prior to the first dipole intends to match the incoming optical parameters of the positron beam with the optical requirements at the entrance of the FODO lattice. The stability of the FODO lattice is also demonstrated by the periodicity of the β-function from the entrance to the exit of the chicane. As expected, the smallest β_x-function is obtained at the middle of the chicane, simultaneously with the largest dispersion. This allows an efficient momentum collimation.

CHIRP AND COMPRESSION

The second chicane intends to compress longitudinally the beam. To reach an efficient compression, a correlation between $\delta p/p$ and z is introduced by chirping the beam with an RF cavity. A second requirement is a magnetic chicane with appropriate properties to link the momentum dispersion to the longitudinal bunch length. The compression factor for a small momentum dispersion can be written as

$$C = \frac{1}{1 + \kappa R_{56}} \tag{3}$$

where R_{56} is the matrix element 56 of the chicane transfer matrix. It controls the longitudinal size of the beam according to

$$\Delta z = R_{56} \left.\frac{\delta p}{p}\right|_{in} \tag{4}$$

where $(\delta p/p)_{in}$ represents the initial longitudinal momentum spread, and κ characterizes the beam chirp created by the cavity. The latter can be expressed as

$$\kappa = \frac{d}{dz}\frac{\delta p}{p} = \frac{2\pi f}{c}\frac{eV_0}{E_0 + eV_0\cos\phi}\sin\phi \tag{5}$$

where f is the cavity frequency (Hz), eV_0 is the cavity acceleration (MeV), E_0 is the central energy (MeV), and ϕ is the cavity phase advance. Fig. 5 shows the compression factor peak at ϕ=-96.6° (left), which describes the setting of the cavity with a proper chirp. The effect of full system on the $(\delta p/p, t)$ beam profile, including the appropriate R_{56} chicane, exhibits a beam length at the exit of the chicane 23 times smaller than the entrance ones (Fig. 5 right).

CONCLUSION

The generation and injection of cw positron beams suitable to the high performance will present a number of technical challenges which must be overcome. One of the challenges is to decrease the momentum dispersion of the collimated positron distribution from $\delta p/p$=±10% to ±2%. A set of cavities at the exit of the first chicane will serve this purpose, and acceleration through the south linac will provide about ten times further reduction. The CEBAF arcs can also be tuned for more compression providing an additional chirp. An optimization will be performed to obtain a reduction factor suitable for CEBAF acceptances that are a bunch length of Δt=4 ps and amomentum spread of $\delta p/p$=±2%. Further studies about the capture magnet are also foreseen as different magnets may support different operation mode. The concept optimization is being explored with further analytical and simulation studies. Further, a new positron injector may be assembled at the Low Energy Research Facility (LERF) to develop a proof-of-principle, and then later maybe connected to the CEBAF accelerator through a new transport line.

ACKNOWLEDGMENTS

This material is based upon work supported by the U.S. Department of Energy, Office of Science, Office of Nuclear Physics under contract DE-AC05-06OR23177. This work has received funding from the European Union's Horizon 2020 research and innovation program under grant agreement No 824093.

REFERENCES

[1] E. Voutier. "Physics potential of polarized positrons at the Jefferson Laboratory." In: *Nucl. Theor.* 33 (2014).

Ed. by A. Georgieva and N. Minkov, pp. 142–151. arXiv: 1412.1249 [nucl-ex].

[2] N. Alamanos, M. Battaglieri, D. Higinbotham, S. Niccolai, A. Schmidt, E. Voutier. "Topical issue on an experimental program with positron beams at Jefferson Lab." In: *Eur. Phys. J. A* 58.3 (2022), p. 45. DOI: 10.1140/epja/s10050-022-00699-6.

[3] A. Accardi et al. "An experimental program with high duty-cycle polarized and unpolarized positron beams at Jefferson Lab." In: *Eur. Phys. J. A* 57.8 (2021), p. 261. DOI: 10.1140/epja/s10050-021-00564-y. arXiv: 2007.15081 [nucl-ex].

[4] J. Grames, E. Voutier et al. "Polarized Electrons for Polarized Positrons: a proof–of–principle experiment." Jefferson Lab Experiment **E12-11-105**. 2012.

[5] E. Voutier. "The PEPPo Concept for a Polarized Positron Source." In: *4th International Particle Accelerator Conference*. 2013, WEOAB203.

[6] D. Abbott et al. "Production of Highly Polarized Positrons Using Polarized Electrons at MeV Energies." In: *Phys. Rev. Lett.* **116** (21 2016), p. 214801.

[7] R. Boni, S. Guiducci, and M. Vescovi. "A new system for positron focusing at the Frascati LinAc." In: (Jan. 1981).

[8] S. Agostinelli et al. "GEANT4–a simulation toolkit." In: *Nucl. Instrum. Meth. A* 506 (2003), pp. 250–303. DOI: 10.1016/S0168-9002(03)01368-8.

[9] H. Wiedemann. *Particle Accelerator Physics*. SpringerLink: Springer e-Books. Springer Berlin Heidelberg, 2007. ISBN: 9783540490456. URL: https://books.google.com/books?id=S8CfmLe87RAC.